

# Direct-Photon Production from SPS to RHIC Energies

Klaus Reygers<sup>1</sup> for the PHENIX collaboration

Institut für Kernphysik, University of Münster, Germany

Received: date / Revised version: date

**Abstract.** Direct photons are an important tool for the detection of the quark-gluon plasma in ultra-relativistic nucleus-nucleus collisions. Direct-photon measurements were made in Pb+Pb collisions at  $\sqrt{s_{NN}} = 17.2$  GeV and in Au+Au collisions at  $\sqrt{s_{NN}} = 200$  GeV. These results are reviewed and compared with model calculations.

**PACS.** PACS-key describing text of that key – PACS-key describing text of that key

## 1 Introduction

Measurements of direct photons, *i.e.* of photons which are not produced in electromagnetic decays like  $\pi^0 \rightarrow \gamma + \gamma$  and  $\eta \rightarrow \gamma + \gamma$ , have a long history [1,2]. First measurements of direct photons in proton-proton collisions were made in the late 1970's and hinted at the presence of point-like charged objects within the proton. Quantum chromodynamics (QCD) was developed at this time and made predictions for direct-photon production. The experimental test of QCD became the primary motivation for direct-photon measurements. QCD is now considered the correct theory of the strong interaction and the focus of direct-photon measurements in collisions of hadrons has shifted towards constraining the gluon distribution function within hadrons. Direct photons are specially suited for this because gluons are involved at leading order in photon production via the quark-gluon Compton scattering ( $q + g \rightarrow q + \gamma$ ) whereas gluons are involved only at next-to-leading order in processes like deep inelastic scattering of leptons.

The interest in direct photons in collisions of heavy nuclei arises from the fact that once they are produced photons leave the hot and dense fireball virtually without further interaction. They can thus convey information about the early stage of a nucleus-nucleus collision. It is expected that in the early stage of a nucleus-nucleus collision with sufficiently high energy a thermalized medium is formed in which quarks and gluons are the relevant degrees of freedom. The electric charges in such a quark-gluon plasma (QGP) are expected to radiate photons whose momentum distribution reflects the temperature of the system. The production of thermal photons was suggested as a QGP signature [3,4]. The fireball produced in a nucleus-nucleus collision expands and cools. The dominant contribution to the spectrum of thermal direct photons is expected from the early hot phase directly after thermalization. Thus, by

measuring thermal direct photons one can constrain the initial temperature of the fireball.

The transverse momentum spectrum of thermal photons is expected to decrease approximately as  $\exp(-p_T/T)$  for temperature  $T$ . Direct photons from initial parton-parton scatterings with high momentum transfer (hard scattering) follow a power-law shape  $p_T^{-n}$  and thus dominate the direct-photon spectrum at sufficiently high  $p_T$ . This is schematically shown in Figure 1. The measurement of direct photons at high  $p_T$  in nucleus-nucleus collisions allows to test the expected scaling of particle yields in hard processes with the number of inelastic nucleon-nucleon collisions ( $N_{coll}$ ). This is of paramount importance for the interpretation of the suppression of hadrons at high- $p_T$  in central Au+Au collisions at RHIC as a final state effect, *i.e.* as an effect that is caused by the medium created in those collisions. A common interpretation is that high- $p_T$  hadron suppression is the result of energy loss of partons in the medium after their initial hard scattering (jet quenching) [5].

## 2 Production Mechanisms

For the production of direct photons in collisions of hadrons complete next-to-leading order (NLO) calculations in perturbative QCD (pQCD) are available. In these calculations the total direct-photon cross section can be considered as the sum of a direct component and a bremsstrahlung component [6]:

$$\sigma_{tot}^{direct\gamma} = \sigma_{direct} + \sigma_{brems}. \quad (1)$$

The dominant contributions to the direct component come from quark-antiquark annihilation ( $q + \bar{q} \rightarrow g + \gamma$ ) and quark-gluon Compton scattering ( $q + g \rightarrow q + \gamma$ ). The bremsstrahlung component contains calculable processes in which a photon is radiated off a quark (*e.g.*  $q + g \rightarrow$

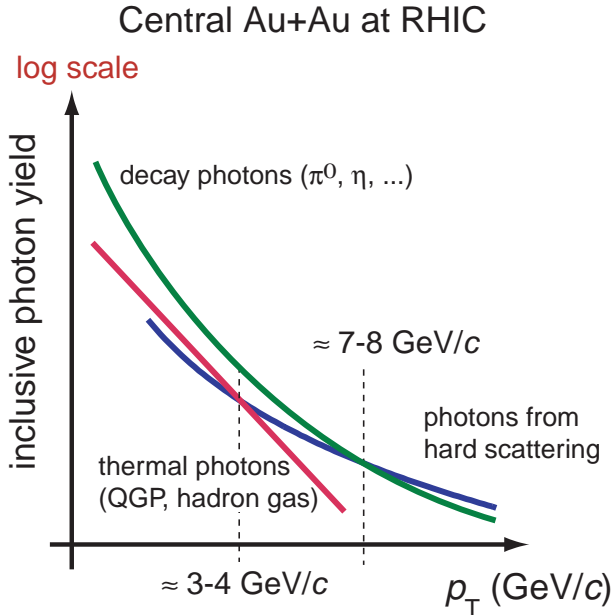


**Fig. 1.** Schematic representation of the different contributions to the inclusive photon spectrum in Au+Au collisions at RHIC. Over a wide transverse momentum range thermal direct photons from the QGP and the hadron gas as well as prompt photons from initial hard parton scattering are overwhelmed by photons from hadron decays. The strong suppression of neutral pions and  $\eta$  mesons in central Au+Au collisions at RHIC ( $\sqrt{s_{NN}} = 200 \text{ GeV}$ ) results in a reduced decay photon background and eases the extraction of a direct-photon signal.

$q + g + \gamma$ ) but also photons produced in the fragmentation of quarks and gluons into hadrons. The latter process is a soft process that cannot be described by pQCD and is therefore described by a phenomenological parton-to-photon fragmentation function.

An intrinsic uncertainty in the pQCD calculation arises due to the choice of unphysical and arbitrary renormalization, factorization, and fragmentation scales. The resulting uncertainties of the calculated direct-photon transverse momentum ( $p_T$ ) spectra are typically on the order of 20-30% [6]. The comparison of data and pQCD calculations in  $p + p(\bar{p})$  collisions over a wide range of collision energies ( $\sqrt{s}$ ) shows a systematic pattern of deviation: the measured direct-photon  $p_T$  distributions are typically steeper than the QCD prediction and so in many comparisons the measured direct-photon yields at low- $p_T$  lie above the QCD expectations [7]. With a non-perturbative parameter  $k_T$ , which reflects an initial state transverse momentum component of the partons prior to the hard scattering, it is possible to improve the agreement between data and QCD.

In ultra-relativistic collisions of nuclei additional direct-photon sources are expected. One generally distinguishes between thermal and non-thermal direct photons. Non-thermal direct photons include prompt (or pQCD) photons, which result from hard initial parton-parton scattering analogous to the production mechanism in  $p + p(\bar{p})$  collisions. Due to intense rescattering among the quarks

and gluons produced in a nucleus-nucleus collision one expects that a thermalized QGP is formed after a formation time  $\tau_0$ . Pre-equilibrium direct photons produced after the initial parton-parton scattering but before thermalization are a second source of non-thermal photons. So far the theoretical description of pre-equilibrium direct-photon production is not well under control. The QGP expands and cools and at temperature of  $T_c \approx 170 \text{ MeV}$  a transition to a gas of hadrons is expected [8]. Thermal direct photons are both produced in the QGP phase and in the hadron-gas phase. The production of direct photons per unit time and volume for a given temperature has been calculated for a QGP and for a hadron gas [9,10]. These state-of-the-art results indicate that at the same temperature the photon production rates in a QGP and a hadron gas are very similar. The photon rates must be convoluted with the space-time evolution of the fireball in order to obtain prediction for thermal photon production in nucleus-nucleus collisions. Pure hadron gas scenarios and scenarios with phase transition can be compared to data in order to make statements about the formation of a QGP in these collisions.

Besides thermal and non-thermal direct photons a third category of hard+thermal photons is conceivable in nucleus-nucleus collisions. It was suggested that a significant number of direct photons results from processes in which a fast parton from initial hard scattering interacts with a thermalized parton of the QGP [11]. These processes include Compton scattering ( $q_{\text{hard}} + g_{\text{QGP}} \rightarrow \gamma + q$ ) and annihilation ( $q_{\text{hard}} + \bar{q}_{\text{QGP}} \rightarrow \gamma + g$ ). Recently, it was pointed out that also induced photon bremsstrahlung from multiple scattering of a fast quark in a QGP might be a significant source of direct photons [12]. The process is similar to medium induced gluon emission which is the dominant energy loss mechanism for fast quarks in a QGP.

### 3 Measurement of Direct Photons

The direct-photon measurements presented here were made with highly segmented electro-magnetic calorimeters. In low-multiplicity environments, as *e.g.*  $p + p$  or  $p + \bar{p}$  collisions, one can considerably reduce the decay photon background by accepting only those hits as direct-photon candidates which don't form an invariant mass in the mass range of the  $\pi^0$  or  $\eta$  meson with other photon hits in the same event. Moreover, direct photons produced in these collisions via a direct production mechanism, whose momentum is therefore balanced by a particle jet on the away side, can be identified by so-called isolation cuts which set a limit on the sum of the energies of particles in a cone around the photon. Due to the high multiplicity of produced particles it is difficult to apply such cuts in central collisions of heavy nuclei.

The first step in the measurement direct photons in nucleus-nucleus collisions is the measurement of the inclusive photon  $p_T$  spectrum, *e.g.* of the spectrum that includes direct photons as well as decay photons. The fraction of charged particle background hits is usually measured and subtracted with the aid of position sensitive

detectors located directly in front of the calorimeter. A correction for the contribution of fake photon hits produced by neutrons and antineutrons, which cannot be determined experimentally, is obtained on the basis of detailed Monte-Carlo simulations. The second step is an accurate measurement of the  $p_T$  spectrum of neutral pions and  $\eta$  mesons with the same detector. Based on these spectra the expected decay photons are calculated. This is usually done with Monte-Carlo calculations which also take into account the small contribution from other hadrons (*e.g.*  $\eta'$ ,  $\omega$ ) with a decay branch into photons. Since the high- $p_T$  part of the  $\pi^0$  spectrum in a nucleus-nucleus collision can be described by a power-law and the dominant contribution to the decay-photon background comes from  $\pi^0$  decays, the following formula is a useful estimate of the background photons per  $\pi^0$ :

$$\frac{1}{p_T} \frac{dN_{\pi^0}}{dp_T} \propto p_T^{-n} \Rightarrow \frac{\gamma_{\pi^0}^{\text{decay}}}{\pi^0} \approx \frac{2}{n-1}. \quad (2)$$

At RHIC energies the high- $p_T$   $\pi^0$  spectrum can be described with  $n \approx 8$ , so that at a given  $p_T$  one roughly expects  $\gamma_{\pi^0}^{\text{decay}}/\pi^0 \approx 0.28$  decay photons per neutral pion.

The final step in the determination of the direct-photon spectrum is the subtraction of the calculated decay photon spectrum from the inclusive photon spectrum. The invariant direct-photon yield  $\gamma_{\text{direct}} \equiv E d^3N/d^3p$  is calculated as a fraction of the inclusive photon spectrum:

$$\gamma_{\text{direct}} = \gamma_{\text{incl}} - \gamma_{\text{decay}} = \left(1 - \frac{\gamma_{\text{decay}}}{\gamma_{\text{incl}}}\right) \cdot \gamma_{\text{incl}} \quad (3)$$

$$\equiv (1 - R_\gamma^{-1}) \cdot \gamma_{\text{incl}}, \quad (4)$$

where

$$R_\gamma = \frac{\gamma_{\text{incl}}}{\gamma_{\text{decay}}} \approx \frac{(\gamma_{\text{incl}}/\pi^0)_{\text{meas}}}{(\gamma_{\text{decay}}/\pi^0)_{\text{calc}}}. \quad (5)$$

The double ratio as given by the rightmost expression in Eq. 5 is used to calculate  $R_\gamma$  because in the ratio  $(\gamma_{\text{incl}}/\pi^0)_{\text{meas}}$  correlated systematic uncertainties of the photon and  $\pi^0$  measurement partially cancel. The systematic uncertainties related to the energy scale of the detector and to corrections which take detector effects like energy smearing and shower overlap into account are examples for such correlated systematic uncertainties. The ratio  $(\gamma_{\text{decay}}/\pi^0)_{\text{calc}}$  is the result of the (Monte-Carlo) calculation of the expected background decay photons from  $\pi^0$ ,  $\eta$  and other hadron decays per neutral pion.  $R_\gamma$  contains the entire statistical and systematic significance of the direct-photon signal. In the calculation of the respective direct-photon  $p_T$  spectrum only those systematic uncertainties that canceled in the double ratio must be added.

## 4 CERN SPS Results

Early attempts to measure a direct-photon signal in fixed-target experiments with proton, oxygen, and sulfur beams at a beam energy of 200 GeV per nucleon at the CERN SPS resulted in upper limits on the direct-photon signal.

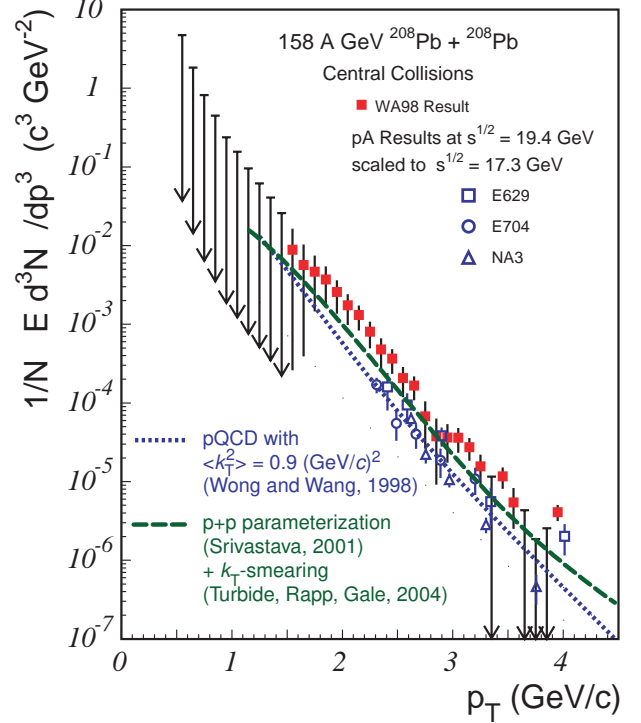


**Fig. 2.** The invariant direct-photon multiplicity as a function of the transverse momentum  $p_T$  in central Pb+Pb collisions at  $\sqrt{s_{NN}} = 17.2$  GeV. The central event class corresponds to 0 – 12.7% of the WA98 minimum bias trigger which in turn corresponds roughly to 0 – 11% of the inelastic Pb+Pb cross section. The error bars indicate combined statistical and systematic uncertainties. The upper edges of the arrows represent 90% C.L. upper limits on the direct-photon yield. The WA98 data points are compared with scaled p+p and p+C results, pQCD calculation which include  $k_T$  broadening, and scaled parameterizations of direct-photon yields in p+p collisions.

At moderate transverse momenta ( $p_T \gtrsim 0.5$  GeV/c) upper limits on  $(\gamma_{\text{direct}}/\gamma_{\text{decay}})$  on the order of 15% were determined [13,14,15,16]. The WA80 experiment found an (non-significant) average direct-photon excess in central  $^{32}\text{S}+\text{Au}$  collisions in the range  $0.5 \text{ GeV}/c \leq p_T \leq 2.5 \text{ GeV}/c$  of  $5.0\% \pm 0.8\%(\text{stat}) \pm 5.8\%(\text{syst})$ . Comparisons with theoretical calculations showed that the respective  $p_T$  dependent upper limits were consistent with scenarios with a phase transition as well as with scenarios without a phase transition [17].

The first significant direct-photon signal in ultra-relativistic nucleus-nucleus collisions was found at the CERN SPS by the fixed-target experiment WA98 in Pb+Pb collisions at a beam energy of 158 GeV per nucleon corresponding to a center-of-mass energy of  $\sqrt{s_{NN}} = 17.2$  GeV per nucleon-nucleon pair [18]. A direct-photon signal of about  $\gamma_{\text{direct}}/\gamma_{\text{decay}} \approx 20\% \pm 9\%(\text{syst})$  in the range  $p_T \gtrsim 2$  GeV/c was found in central Pb+Pb collisions. No significant signal was observed in peripheral collisions. The extracted invariant direct-photon yield for central Pb+Pb collisions is shown in Figure 2.

The obvious question is whether the direct-photon spectrum in central Pb+Pb collisions can be explained simply by hard scattering processes or whether an additional thermal component is necessary. A first step towards answering this question is the comparison of the WA98 results with p+p and p+C results scaled by the average number of inelastic nucleon-nucleon collision ( $\langle N_{\text{coll}} \rangle \approx 660$ ) for the central Pb+Pb class. A systematic uncertainty results from the fact that the p+p and p+C data were measured at  $\sqrt{s_{\text{NN}}} = 19.4$  GeV and therefore need to be scaled down to  $\sqrt{s_{\text{NN}}} = 17.2$  GeV assuming scaling in  $x_{\text{T}} = 2p_{\text{T}}/\sqrt{s_{\text{NN}}}$ . Figure 2 shows that the scaled p+p and p+C results lie systematically below the Pb+Pb data which suggests nuclear effects beyond the simple  $N_{\text{coll}}$  scaling of the direct-photon yields. Since no p+A data are available for  $p_{\text{T}} < 2.5$  GeV/c the Pb+Pb results are compared to a p+p pQCD calculation [19] and to a parameterization of direct-photon yields in p+p collisions [10], both scaled by  $N_{\text{coll}}$ . With a transverse momentum broadening of  $\langle k_{\text{T}}^2 \rangle = 0.9$  GeV<sup>2</sup> the pQCD calculation offers a good description of the p+A data. By contrast, the Pb+Pb data for  $p_{\text{T}} \lesssim 2.5$  GeV/c are noticeably above the pQCD expectation. The parameterization of the direct-photon yields shown in Figure 2 is the parameterization from [20], modified according to the additional  $k_{\text{T}}$  broadening expected in nuclear targets (Cronin effect) [10]. This parameterization hardly gives a satisfactory descriptions of the Pb+Pb data which hints at the presence of thermal photon sources in Pb+Pb collisions. The effect of nuclear  $k_{\text{T}}$  broadening on the direct-photon yield was systematically studied in [21]. The authors conclude that regardless of the amount of  $k_{\text{T}}$  broadening that is assumed in their calculations the Pb+Pb data in the range  $p_{\text{T}} \lesssim 2.5$  GeV/c cannot be described by leading-order pQCD. Thus, it appears unlikely that the WA98 data can be described by hard scattering processes alone. Firmer conclusions, however, can only be drawn with better p+p and p+A reference data.

A striking feature of the WA98 data becomes visible in Figure 3 which shows the  $\gamma_{\text{direct}}/\pi^0$  ratio as a function of  $p_{\text{T}}$  for central Pb+Pb collisions along with the p+p and p+C reference data. For  $p_{\text{T}} \gtrsim 2.5$  GeV/c the Pb+Pb and p+A results are in agreement. The solid line represents a fit to the p+A data with a functional form which can well describe the  $\gamma_{\text{direct}}/\pi^0$  obtained in pQCD calculations. In the range  $1.5$  GeV/c  $< p_{\text{T}} < 2.5$  GeV/c the Pb+Pb data exhibit a characteristic deviation from the solid line which reflects the expected behavior for direct photon and neutral pion production in hard scattering processes. A possible explanation for this observation is the production of thermal direct photons in central Pb+Pb collisions at the CERN SPS.

Several authors have calculated the expected direct-photon spectrum in central Pb+Pb collisions at the CERN SPS in scenarios in which thermal photons are produced in a QGP and in a hadron gas in addition to prompt direct photons. In some of these models the evolution of the reaction zone is determined with hydrodynamic calculations, other models employ simple parameterizations

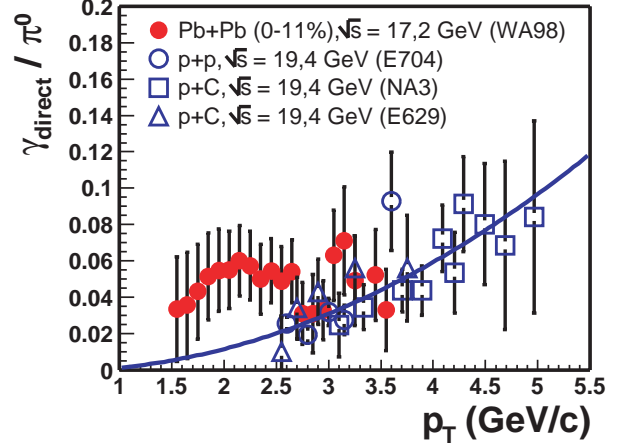


**Fig. 3.** Invariant direct-photon multiplicity divided by the invariant neutral pion multiplicity for p+A and central Pb+Pb collisions as a function of transverse momentum. No  $x_{\text{T}}$  scaling of the p+A yields was applied here. The solid line represents a fit to the p+A data with a functional form which can well describe the  $\gamma_{\text{direct}}/\pi^0$  obtained in pQCD calculations.

of the fireball evolution. One objective of these model comparisons is the determination of the initial temperature of the fireball directly after thermalization. In [10] it was shown that in the absence of additional nuclear  $k_{\text{T}}$  broadening (*i.e.* in the absence of the Cronin effect) the WA98 data can be described with an initial temperature of  $T_i = 270$  MeV in a scenario with phase transition from a QGP to a hadron gas. However, if nuclear  $k_{\text{T}}$  broadening is assumed ( $\langle \Delta k_{\text{T}}^2 \rangle = 0.2$  GeV<sup>2</sup>) the data can be well described with a much lower initial temperature of  $T_i = 205$  MeV. For the latter case the different contributions to the calculated spectrum and the comparison of the sum of all contributions with the WA98 data are shown in Figure 4.

According to [22] the WA98 data suggest a very small formation time  $\tau_0 \approx 0.2$  fm/c and a high initial temperature on the order of  $T_i \approx 335$  MeV. In [23] the WA98 data are found to be consistent with initial temperatures in the range  $250$  MeV  $\lesssim T_i \lesssim 370$  MeV. In [24] the data are compared with hydrodynamic calculations with and without a QGP phase. In both scenarios the authors can describe the data with initial temperatures between  $210$  MeV  $\lesssim T_i \lesssim 260$  MeV. Thus, one can conclude that the WA98 data can be naturally explained in a QGP scenario but don't offer a direct proof for the existence of this state of matter. Unfortunately there are large variations in the extracted initial temperatures but one should also note that most models suggest initial temperatures  $T_i$  above the critical temperature  $T_c$  for the QGP phase transition.

The method of measuring direct photons by subtracting the expected decay-photon yield from the measured inclusive yield depends on the accurate measurement of the  $\pi^0$   $p_{\text{T}}$  spectrum. Largely due to systematic uncertainties of the  $\pi^0$  measurement at low  $p_{\text{T}}$  no significant direct-photon signal could be observed with the subtraction method in central Pb+Pb collisions for  $p_{\text{T}} < 1.5$  GeV/c. An alterna-

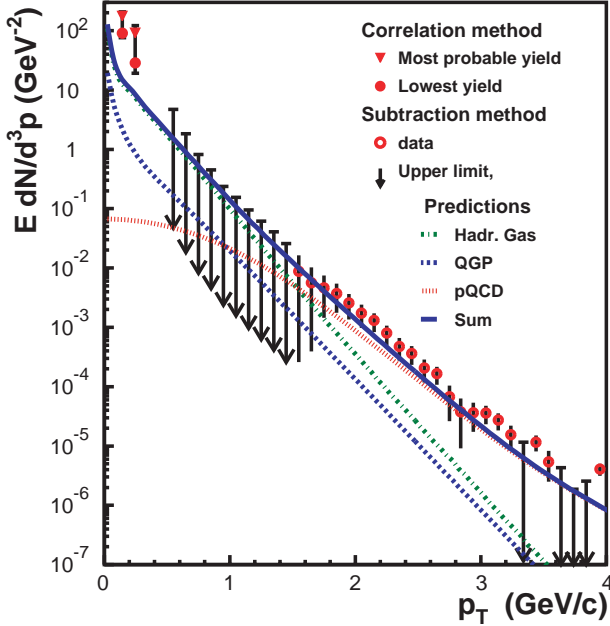


**Fig. 4.** Comparison of the WA98 data with a model calculation [10] which includes a phase transition from a QGP to a hadron gas. The data points at low  $p_T$  obtained from Hanbury Brown-Twiss interferometry cannot be explained by this calculation.

tive method of extracting the direct-photon yield is based on Bose-Einstein two-particle correlations of direct photons at small relative momenta which is absent for photons from hadron decays. This method requires a very good understanding of background effects which could mimic two-photon correlations. These effects include splitting of single particle showers into two nearby clusters, misidentification of  $e^+e^-$ -pairs from photon conversion as photon hits, and Bose-Einstein correlations of charged pions misidentified as photons. In addition to the expected background effects the WA98 experiment observed genuine two-photon correlations which were attributed to Bose-Einstein correlations [25]. From the observed correlation strength it was possible to determine the direct-photon yield in the range  $0.1 \text{ GeV}/c < p_T < 0.3 \text{ GeV}/c$ . The new data points are compared to a theoretical calculation in Figure 4. The measured direct-photon yields exceed this model calculation which attributes the dominant contribution in this  $p_T$  range to direct photons from the hadron gas phase.

## 5 RHIC Results

By comparing the measured inclusive photon  $p_T$  spectrum with the expected photons from hadron decays the PHENIX experiment was able to observe a direct-photon signal in Au+Au collisions at  $\sqrt{s_{NN}} = 200 \text{ GeV}$  up to transverse momenta of  $p_T \approx 12 \text{ GeV}/c$  [26]. PHENIX employed two different types of highly segmented electromagnetic calorimeters: a lead-scintillator sandwich calorimeter (PbSc) and a leadglass Cherenkov (PbGl) calorimeter. The independent direct-photon measurements made

with these two detectors, which have a different response to hadrons, were found to be in agreement. The PbSc and PbGl results were averaged in order to reduce the statistical uncertainty of the direct-photon signal. Figure 5 shows the ratio  $R_\gamma$  of the measured inclusive photons to the expected decay photons in central Au+Au collisions. A significant direct-photon signal is visible for  $p_T \gtrsim 4 \text{ GeV}/c$ . Above  $p_T \approx 7 \text{ GeV}/c$  the number of direct photons exceeds the number of photons from hadron decays.

In the  $p_T$  range where the photon excess is observed direct photons are expected to result from initial hard parton-parton scatterings which can be described by pQCD. Neutral pions and charged hadrons at high  $p_T$  in central Au+Au collisions at RHIC were found to be suppressed relative to the cross section in p+p collisions scaled by a geometrical factor  $\langle T_{AB} \rangle_f \equiv \langle N_{\text{coll}} \rangle / \sigma_{\text{inel}}^{\text{p+p}}$  [27]. This  $N_{\text{coll}}$  scaling is only expected for hard-scattering processes. The high- $p_T$  hadron suppression can be explained by energy loss of fast partons from initial hard scatterings in the medium of high color charge density produced in Au+Au collisions. Thus, in this picture the hadron suppression is attributed to a final state effect. Alternative models suggested that the hadron suppression is related to an initial state effect, namely to special properties of the gluon densities in the ground state Au nucleus [28]. High- $p_T$  direct photon and *e.g.* neutral pion production in Au+Au collisions are sensitive to the same initial flux of incoming partons. High- $p_T$  direct photons, however, are largely unaffected by the created hot and dense medium.

In Figure 5 the measured direct-photon signal is compared to the expected signal in case  $N_{\text{coll}}$  scaling of the direct-photon multiplicities holds for Au+Au collisions. The solid line represents the ratio

$$\frac{\gamma_{\text{incl}}^{\text{Au+Au}}}{\gamma_{\text{decay}}^{\text{Au+Au}}} = \frac{\gamma_{\text{direct}}^{\text{Au+Au}} + \gamma_{\text{decay}}^{\text{Au+Au}}}{\gamma_{\text{decay}}^{\text{Au+Au}}} = 1 + \frac{\langle N_{\text{coll}} \rangle \cdot \gamma_{\text{direct}}^{\text{p+p}}}{\gamma_{\text{decay}}^{\text{Au+Au}}}. \quad (6)$$

The result of a NLO pQCD calculation [29,30] was used as p+p direct-photon reference ( $\gamma_{\text{direct}}^{\text{p+p}}$ ). Comparisons with final direct-photon data for p+p collisions at  $\sqrt{s} = 200 \text{ GeV}$  from RHIC Run-2 [31] and preliminary results from Run-3 [32] justify the use of the pQCD calculation as a reference. The intrinsic uncertainty of the pQCD photon yield ( $\approx 20\%$ ) due to the choice of the QCD scales is not shown. The agreement of the solid line in Figure 5 with the data point shows that in central Au+Au collisions at RHIC high- $p_T$  direct photons are not suppressed and follow  $N_{\text{coll}}$  scaling. The same behavior was also found for less central Au+Au collisions [26]. This shows that the observed suppression of hadrons at high  $p_T$  is due to final state effects and therefore supports the interpretation of the hadron suppression as the result of jet-quenching.

According to the calculation in [10] thermal direct photons from a QGP produced in central Au+Au collisions at RHIC might be the dominant direct-photon source in the range  $1 \text{ GeV}/c \lesssim p_T \lesssim 3 \text{ GeV}/c$ . In Figure 5 the expected thermal-photon signal is indicated. This expectation was obtained by adding the ratio of thermal photons (from the QGP and the hadron gas phase) and pQCD photons from

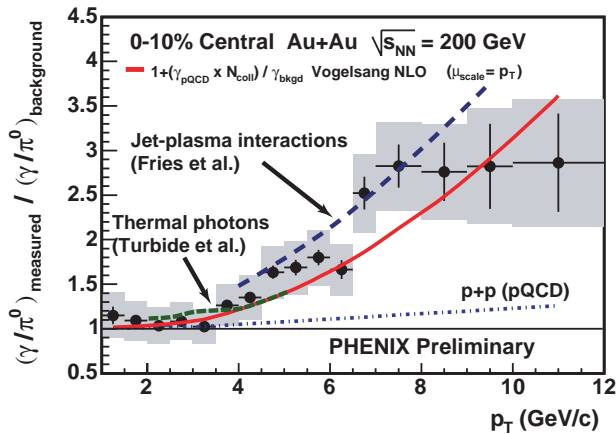


**Fig. 5.** Ratio of the measured inclusive photon spectrum and the expected photon spectrum from the decay of hadrons ( $\pi^0$ ,  $\eta$ , etc.) for central Au+Au collisions at  $\sqrt{s_{NN}} = 200$  GeV. A clear direct-photon signal is visible for  $p_T \gtrsim 4$  GeV/c. The solid line indicates the expected direct-photon excess for the case that the direct photon yield in the Au+Au collisions is given by the direct-photon yield in p+p collisions (at the same energy  $\sqrt{s_{NN}}$ ) scaled by the average number  $\langle N_{coll} \rangle$  of binary nucleon-nucleon collisions for the given Au+Au centrality class. The long dashed line represents the predicted direct-photon signal for a calculation that includes photon production due to the interaction of partons from hard scattering with thermalized partons of the QGP (jet-plasma interactions) [11]. For  $2 \text{ GeV}/c < p_T < 5 \text{ GeV}/c$  an estimate of the expected thermal photon signal is compared to the data.

[10] to the pQCD curve (solid line) shown in Figure 5. This estimate illustrates that the expected signal from thermal direct photons is rather small (on the order of 10%). With the current systematic uncertainties no statement can be made about the presence of thermal direct photons.

Figure 5 furthermore shows an estimate of the direct-photon signal in central Au+Au collisions at RHIC in case jet-plasma interactions as calculated in [11] contribute to the direct-photon production (long dashed line). The ratio of photons from the interaction of fast quarks from hard scattering with the QGP and photons from (leading-order) pQCD determined in [11] was added to the (next-to-leading order) pQCD curve (solid line) in Figure 5. The leading order photon calculation in [11] doesn't include a  $K$  factor which can be used to account for higher order contributions. In [21] the leading order direct photon spectra were *e.g.* multiplied by a factor  $K = 2$ . Therefore, the result in the presence of jet-plasma interactions is only a rough estimate. It shows, however, that with the uncertainties of the preliminary PHENIX data it is not possible to decide whether there's a strong contribution of photons from jet-plasma interactions. In non-central nucleus-nucleus collisions the path length of a parton from hard scattering depends on the angle with respect to the reaction plane and is longest for the direction perpendicular to the reaction plane. Hence, direct photons from jet-plasma interactions should be predominantly produced perpendicular to the reaction plane. This characteristic property

offers an experimental handle on the detection of this photon source.

## 6 Summary

Direct photons in ultra-relativistic collisions of heavy nuclei were observed by the WA98 experiment at the CERN SPS and by the PHENIX experiment at RHIC. The WA98 data can naturally be explained in a QGP scenario. However, also models which don't assume a phase transition to a QGP can describe the data and cannot be ruled out. PHENIX measured direct photons in the high- $p_T$  regime where hard scattering is expected to be the dominant production mechanism. Unlike high- $p_T$  hadrons direct photons are not suppressed in central Au+Au collisions at RHIC. This shows that the suppression of high- $p_T$  hadrons is a final state effect related to properties of the hot and dense medium created in central Au+Au collisions at RHIC.

## References

1. T. Ferbel, W. R. Molzon, *Rev. Mod. Phys.* **56**, 181 (1984).
2. T. Peitzmann, M. H. Thoma, *Phys. Rept.* **364**, 175 (2002).
3. E. L. Feinberg, *Nuovo Cim.* **A34**, 391 (1976).
4. E. V. Shuryak, *Phys. Lett.* **B78**, 150 (1978).
5. I. Vitev, M. Gyulassy, *Phys. Rev. Lett.* **89**, 252301 (2002).
6. P. Aurenche, et al., *Eur. Phys. J.* **C9**, 107 (1999).
7. J. Huston, et al., *Phys. Rev.* **D51**, 6139 (1995).
8. F. Karsch, E. Laermann (2003), [hep-lat/0305025](#).
9. P. Arnold, G. D. Moore, L. G. Yaffe, *JHEP* **12**, 009 (2001).
10. S. Turbide, R. Rapp, C. Gale, *Phys. Rev.* **C69**, 014903 (2004).
11. R. J. Fries, B. Muller, D. K. Srivastava, *Phys. Rev. Lett.* **90**, 132301 (2003).
12. B. G. Zakharov, *JETP Lett.* **80**, 1 (2004).
13. T. Akesson, et al., *Z. Phys.* **C46**, 369 (1990).
14. R. Albrecht, et al., *Z. Phys.* **C51**, 1 (1991).
15. R. Baur, et al., *Z. Phys.* **C71**, 571 (1996).
16. R. Albrecht, et al., *Phys. Rev. Lett.* **76**, 3506 (1996).
17. C. Gale, K. L. Haglin (2003), [hep-ph/0306098](#).
18. M. M. Aggarwal, et al., *Phys. Rev. Lett.* **85**, 3595 (2000).
19. C.-Y. Wong, H. Wang, *Phys. Rev.* **C58**, 376 (1998).
20. D. K. Srivastava, *Eur. Phys. J.* **C22**, 129 (2001).
21. A. Dumitru, et al., *Phys. Rev.* **C64**, 054909 (2001).
22. D. K. Srivastava (2004), [nucl-th/0411041](#).
23. T. Renk, *Phys. Rev.* **C67**, 064901 (2003).
24. P. Huovinen, P. V. Ruuskanen, S. S. Rasanen, *Phys. Lett.* **B535**, 109 (2002).
25. M. M. Aggarwal, et al., *Phys. Rev. Lett.* **93**, 022301 (2004).
26. J. Frantz, et al., *J. Phys.* **G30**, S1003 (2004).
27. K. Adcox, et al. (2004), [nucl-ex/0410003](#).
28. D. Kharzeev, E. Levin, L. McLerran, *Phys. Lett.* **B561**, 93 (2003).
29. L. E. Gordon, W. Vogelsang, *Phys. Rev.* **D48**, 3136 (1993).
30. L. E. Gordon, W. Vogelsang, *Phys. Rev.* **D50**, 1901 (1994).
31. S. Adler, et al. (2005), [hep-ex/0502006](#).
32. K. Okada, et al. (2005), [hep-ex/0501066](#).